



# A review of friction laws and their application for simulation of microseismicity prior to hydraulic fracturing

Jiyang Ye, Mirko Van Der Baan

(Email: [jiyang1@ualberta.ca](mailto:jiyang1@ualberta.ca), [Mirko.VanderBaan@ualberta.ca](mailto:Mirko.VanderBaan@ualberta.ca))

Dept. of Physics, CCIS, University of Alberta, T6G 2E1, Canada

## Summary

Using geomechanical models to predict the location of microseismicity before the hydraulic stimulation is useful for both effective production and safety. After building the mechanical earth model, the application of the appropriate initiation and propagation criteria is a critical step for correctly predicting the temporal evolution and location of failure and thus the microseismicity. For simplicity we focus on shear events only which are governed by the Mohr-Coulomb criterion describing initiation, propagation and termination of failure. We introduce three different friction laws, and then compare predicted microseismicity. The friction coefficient is a key parameter. The different friction coefficients cause different rupture processes, in particular if a reduction in driving stress is involved due to lower friction coefficients once slip has initiated. .

## Introduction

Geomechanical modeling plays a key role in understanding the physical mechanisms for microseismicity induced by hydraulic stimulation. Predicting the microseismicity includes two major steps: (1) forward modeling the evolution in static stresses using a hydro-mechanical model and (2) including failure. The physical mechanisms determining static stress changes are relatively well understood but depend on many parameters [Rozhko, 2010; Rutqvist et al., 2008; Segall and Lu, 2015]. Accurately predicting the resulting microseismicity is even more challenging since it introduces dynamic stress changes into the model and feedback mechanisms. It also requires various choices on the most appropriate failure initiation, propagation and termination criteria [Hazzard and Pettitt, 2013; McClure and Horne, 2011].

For simplicity we assume that only shear failure occurs. The failure process can be divided into three steps: initiation, propagation and termination. The Mohr-Coulomb failure criterion is an effective way to determine the instability of a slip in a fault/fracture plane [Scholz, 2002]. It is thus widely used [Hazzard and Pettitt, 2013; McClure and Horne, 2011]. For a given stress state, the key parameter determining initiation, propagation and termination is the frictional coefficient. Many different friction laws have been proposed to describe the evolution of the friction coefficient [Marone, 1998; Scholz, 2002] including constant friction, static-dynamic friction and the rate-and-state friction laws. We investigate the influence of these different friction laws on the predicted microseismicity.

## Mohr-Coulomb failure criterion

The Mohr-Coulomb failure criterion is represented by the equation,

$$\tau = C + \mu(\sigma_n - P) \quad (1)$$

Where  $\tau$  and  $\sigma_n$  are the shear and normal stresses on the fault/fracture plane. The parameter  $\mu$  is called the coefficient of friction,  $C$  is the cohesion,  $P$  is the pore pressure, and the term  $\sigma_n - P$  is the effective normal stress.

Figure 1(a) illustrates the Coulomb failure criterion using a Mohr circle. Increasing the pore pressure  $P$  decreases the effective stress bringing the fracture closer to failure. Likewise decreasing the minimum principal stress or increasing the maximum principal stress also brings the medium closer to failure.

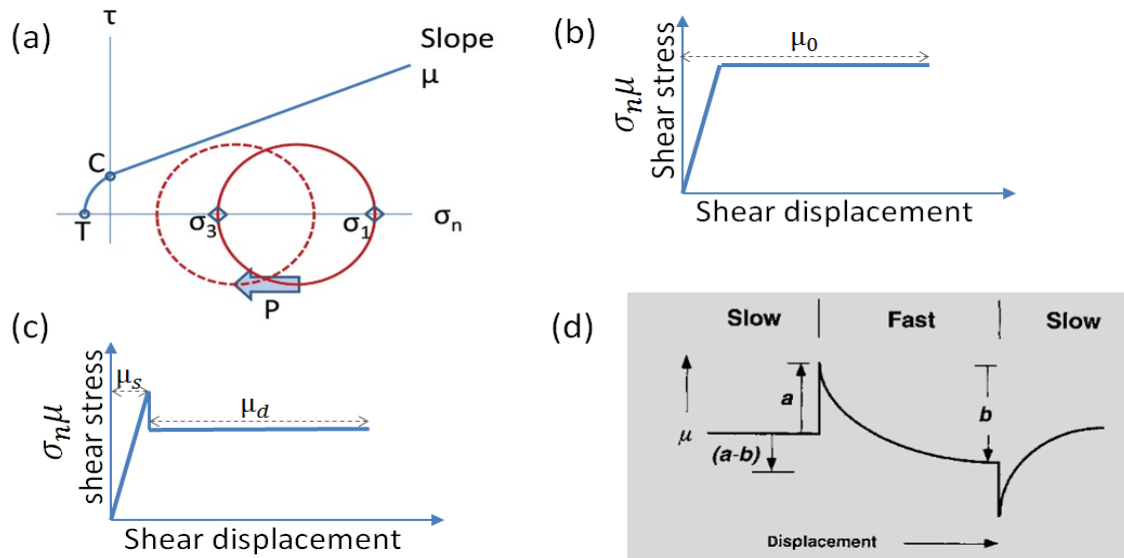


Figure 1. (a) Mohr circle representation of Coulomb failure criterion, from [Maxwell, 2013], (b-c-d) frictional coefficient for constant, static-dynamic and rate-and-state friction law [Scholz, 1998].

### Friction laws

Many friction laws have been introduced to describe the evolution of the friction coefficient.

**Constant friction** - Constant friction is the simplest law, in which the friction coefficient  $\mu = \mu_0$  is a constant. This means that the static (prior to initiation) and dynamic (during propagation/slip) friction coefficients are identical. In other words, slip does not change the friction coefficient (Fig. 1(b)), after slip initiates.

**Static-dynamic friction law** - Based on the static-dynamic friction law, the friction coefficient has two different values namely a dynamic  $\mu_d$  and static  $\mu_s$ , with  $\mu_s > \mu_d$  (Fig. 1(c)). Fracture initiation is determined by the static value  $\mu_s$ ; it reduces to the smaller dynamic value  $\mu_d$  instantaneously when the static frictional resistance is exceeded. If the shear stress drops below the dynamic frictional resistance, slip terminates and the friction coefficient returns to the static value. The last stage is called healing [Hazard and Pettitt, 2013]. That is,

$$\mu = \begin{cases} \mu_d, & \sigma_s \geq \sigma_n \mu_s \\ \mu_s, & \sigma_s < \sigma_n \mu_d \end{cases} \quad (2)$$

Where  $\tau$  and  $\sigma_n$  are the shear and normal stresses on the failure plane.

**Rate-and-state friction law** - Rate-and-state friction law is the leading theory used to describe friction evolution and has been successful in describing a variety of earthquake phenomena [Dieterich, 2007]. The basic idea of this friction law is that the friction coefficient is a function of slip rate and state variable which describes the complex friction memory effects and history dependence [Marone, 1998]. Many different forms of rate-and-state friction law have been used to model laboratory observation of rock friction. The version introduced here is known as the Dieterich-Ruina, and is expressed as [Marone, 1998; Scholz, 2002]

$$\mu = \mu_0 + a \ln \left( \frac{V}{V_0} \right) + b \ln \left( \frac{V_0 \theta}{L} \right) \quad (4)$$

$$\frac{d\theta}{dt} = 1 - \frac{\theta V}{L} \quad (5)$$

Where  $\mu_0$  is a steady-state friction at slip rate  $V_0$ .  $V$  is the slip rate,  $V_0$  is a reference slip rate, and  $a$  and  $b$  are material properties.  $L$  is the critical slip distance and the state variable  $\theta$  evolves according to Eq. (5). Figure 1(d) illustrates the major feature of rate-and-state friction law, a sudden increase in friction of magnitude  $a$ , known as the direct velocity effect, followed by a gradual decrease of friction of magnitude  $b$ .

tude b. The rate-and-state friction law deserves more explanation, and the detailed reviews of rate-and-state friction can be found at [Dieterich, 2007; Marone, 1998; Scholz, 1998].

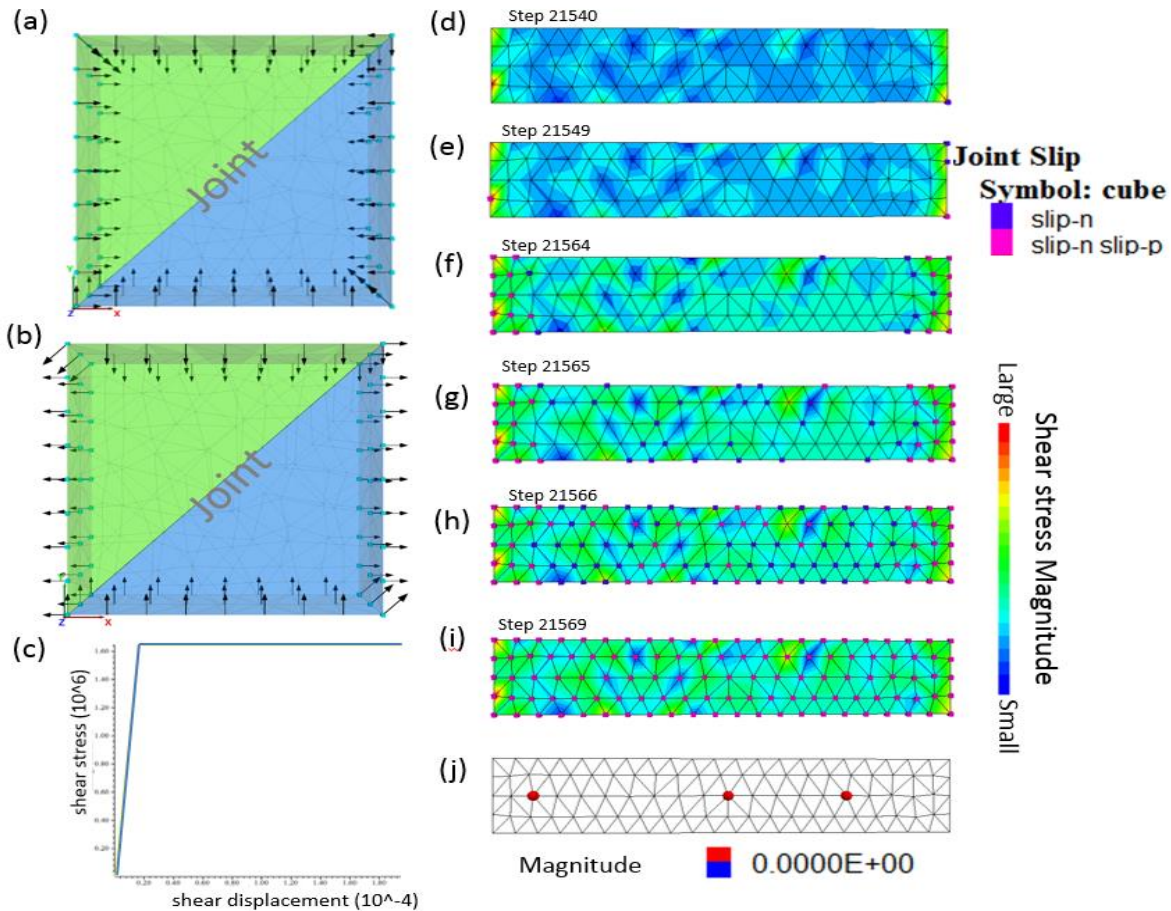


Figure 2. Constant friction law. (a) Initial compressional loading, (b) shear loading, (c) shear stress versus shear displacement for a point in the middle of the joint, (d-i) the magnitude of shear stress represented by the contours and the joint slip status represented by the dots in the joint plane in different steps during the rupture process. Slip-n: slip now; slip-p: slip past. (j) Extracted seismic events from the model.

## Examples

Here, we use three published study cases to effect of different friction laws to predict the microseismicity cloud. Both case 1 and 2 are developed based on [Hazzard and Pettitt, 2013].

### Case 1: Constant friction

Hazzard and Pettitt [2013] simulate the microseismicity due to slip on faults in a distinct element model. It consists of two blocks separated by one fault (labeled 'Joint' in Fig. 2(a)). The model is loaded to a specific normal stress by moving the four outer rectangular boundaries inwards at a constant velocity as the initial stress state (Fig. 2(a)). Next constant shear loading is applied (Fig. 2(b)).

Figure 2(c-j) shows the slip process on the joint using the constant friction coefficient. The shear stress initially accumulates until the frictional strength is exceeded, and then kept constant as indicated by constant friction law (Figure 2c). After initiation of slip at both ends (Fig. 2(d-f)), the elements in the middle starts to slip (Fig. 2(g)), followed by the whole joint slipping (Fig. 2(g)). The constant friction coefficient leads to a simple failure pattern since the amount of shear stress required to keep slip in place does not reduce (Fig 2c). At the last time step the joint reaches a state of stable sliding [Hazzard and Pettitt, 2013]. This leads to only three large magnitude events with an undetermined magnitude since slip is still ongoing (Fig 2j).

### Case 2: Static-dynamic friction

The model setup is the same with case 1 (Figs 2a,b) except a static-dynamic friction coefficient is used. Figure 3 shows the slip rupture processes on the joint. Figure 3(i) shows the shear stress initially accumulates until the frictional strength is exceeded. Once slip occurs the frictional coefficient is reduced to its dynamic value. This leads to a stress drop, reducing the amount of stress required to continue slip. Once slip terminates, healing occurs and the dynamic friction coefficient is reset to its static value, producing a saw tooth pattern in the stress-time curve (Fig3i) [Hazzard and Pettitt, 2013].

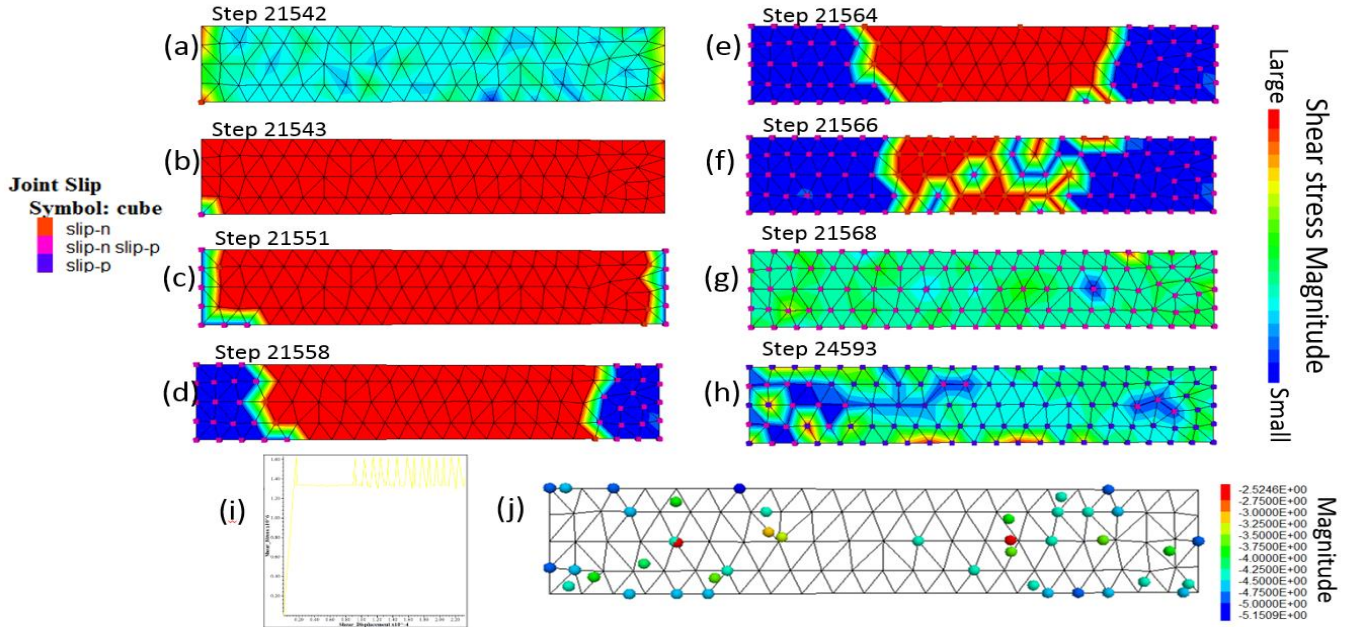


Figure 3. Static-dynamic friction law. (a-h) the magnitude of shear stress represented by the contours and the joint slip status represented by the dots in the joint plane in different steps during the rupture processes. Slip-n: slip now; slip-p: slip past. (i) shear stress versus shear displacement for a point in the middle of the joint, and (j) extracted seismic events from the model.

A static-dynamic friction coefficient leads to a different failure pattern, due to the reduction in required driving stresses. Slip progresses from the ends of the joint towards its center (Fig. 3(a-h)). The reductions in driving stress leads to more but significantly smaller predicted seismic events compared to case 1 (Fig. 2(j)).

### Case 3. Rate-and-state friction coefficient

McClure and Horne [2011] numerically investigate the seismicity induced by injection in a single isolated fracture using rate-and-state friction versus static-dynamic friction [McClure and Horne, 2010]. They find that both friction laws produce similar results with the exception that few low magnitude events occur in the rate and state simulations [McClure and Horne, 2011]. To limit the amount of low magnitude seismic events predicted by static-dynamic friction, [Hazzard and Pettitt, 2013] propose a user threshold, namely the minimum normal stress  $\sigma_n^{min}$  for which slip can be considered a seismic event.

## Conclusions

The friction coefficient is a key parameter greatly influencing the amount and type of predicted microseismicity. In particular, the introduction of static and dynamic friction coefficients can change both the slip and failure patterns since they lead to a reduced driving stress which changes the local stress pattern and subsequently the amount of displacement.

**Acknowledgements** The authors sincerely thank the sponsors of the Microseismic Industry Consortium for financial support and Itasca© for providing licenses to the 3DEC© software. The authors also thank Jim Hazzard for sharing his scripts of microseismicity simulation.

## References

- Dieterich, J. (2007), Applications of rate-and state-dependent friction to models of fault slip and earthquake occurrence, *Treatise on Geophysics*, 4, 107-129.
- Hazzard, J. P., and W. S. Pettitt (2013), Advances in Numerical Modeling of Microseismicity, *47th US Rock Mechanics / Geomechanics Symposium*.
- Marone, C. (1998), Laboratory-Derived Friction Laws and Their Application to Seismic Faulting, *Annual Review of Earth and Planetary Sciences*, 26(1), 643-696.
- Maxwell, S. (2013), Unintentional seismicity induced by hydraulic fracturing, *Canadian Society of Exploration Geophysics Recorder*, 38(8), 40-49.
- McClure, M., and R. N. Horne (2010), Numerical and analytical modeling of the mechanisms of induced seismicity during fluid injection, *GRC Transactions*, 34, 381-396.
- McClure, M., and R. Horne (2011), Investigation of injection-induced seismicity using a coupled fluid flow and rate/state friction model, *Geophysics*, 76(6).
- Rozhko, A. (2010), Role of seepage forces on seismicity triggering, *Journal of Geophysical Research: Solid Earth (1978–2012)*.
- Rutqvist, J., J. T. Birkholzer, and T. Chin-Fu (2008), Coupled reservoir–geomechanical analysis of the potential for tensile and shear failure associated with CO<sub>2</sub> injection in multilayered reservoir–caprock systems, *International Journal of Rock Mechanics and Mining Sciences*.
- Scholz, C. (1998), Earthquakes and friction laws, *Nature*, 391(6662), 37-42.
- Scholz, C. (2002), *The mechanics of earthquakes and faulting*, Cambridge university press.
- Segall, P., and S. Lu (2015), Injection-induced seismicity: Poroelastic and earthquake nucleation effects, *Journal of Geophysical Research: Solid Earth*.